ADVANCES IN ATMOSPHERIC SCIENCES, VOL. 26, NO. 3, 2009, 381–389

Vertical Atmospheric Structure of the Late Summer Clear Days over the East Gansu Loess Plateau in China

WEI Zhigang* (韦志刚), WEN Jun (文 军), and LI Zhenchao (李振朝)

Laboratory for Climate Environment and Disasters of Western China,

Cold and Arid Regions Environmental and Engineering Research Institute,

Chinese Academy of Sciences, Lanzhou 730000

(Received 5 March 2008; revised 15 July 2008)

ABSTRACT

In this paper, by using the sounding data collected in LOPEX05, we have analyzed the vertical atmospheric structure and boundary layer characteristics of temperature and humidity in the late summer over the east Gansu loess plateau. The results show that the bottom of the stratosphere is at about 16 500 m and varies between 14 000 m and 18 000 m above the ground. The center of the westerly jet is located between 8300 m and 14 300 m above the ground and its direction moves between 260° and 305°. There is an inverse humidity layer at about 3000 m height above the ground. The maximum of the air temperature occurs at 1700 LST in the layer below 800 m above the ground. The inversion layer is relatively thick. The time that the maximum of the vapor occurs is not the same for different layers. The depth of the atmospheric boundary layer can reach about 1000 m and the depth of the stable boundary layer can be 650 m.

Key words: atmospheric structure, boundary layer characteristics, the Chinese Loess Plateau

Citation: Wei, Z. G., J. Wen, and Z. C. Li, 2009: Vertical atmospheric structure of the late summer clear days over the east Gansu loess plateau in China. *Adv. Atmos. Sci.*, **26**(3), 381–389, doi: 10.1007/s00376-009-0381-9.

1. Introduction

The Chinese Loess Plateau covers an area of some 626 800 km^2 in the upper and middle parts of the Yellow River (Yang and Shao, 2000). The geomorphic regions of the Loess Plateau are presented in Fig. 1. This mass of loess covers most of Gansu, Shaanxi, Ningxia, Shanxi, and parts of Qinghai, Inner Mongolia, and Henan provinces. The Loess Plateau has been deposited by windstorms in the past and includes a highly erosion-prone soil that is susceptible to the forces of wind and water. Around 40 million people call China's Loess Plateau home.

The Loess Plateau was formed between 2.4 and 1.67 million years ago (Meng and Derbyshire, 1998). It is the world's largest deposit of loess, approximately the size of France. Surrounded by deserts to the north and mountain ranges in all other directions, it has an average thickness of 150 m, extending to 330 m near Lanzhou. The landforms of the Chinese Loess Plateau are very complicated. Mesas, vast ridges, and hemispherical hills are the predominant landforms. The environment has been heavily influenced by the Chinese people for 6 000 years by the growing crops on the Loess Plateau (Doug, 1997). This legacy, combined with overgrazing and a natural climatic trend towards aridity, has all but destroyed the natural vegetation cover of the Loess Plateau (Seth et al., 2000).

In this region, meteorological disasters such as drought, hail, and rainstorm occur frequently and induce serious mountain torrents and mud-rock flows. The precipitation of the Loess Plateau only amounts to an average of 200–550 mm per year. Up to 40% of this annual precipitation has been known to fall in individual storms. These violent rainstorms in the most part occur between July and September. Gullies after such storms appear in the Plateau, as the rainwater pushes easily through the fine dust and makes its way to the tributaries of the river. The weather and climatic variations influence obviously social and

*Corresponding author: WEI Zhigang, wzg@lzb.ac.cn

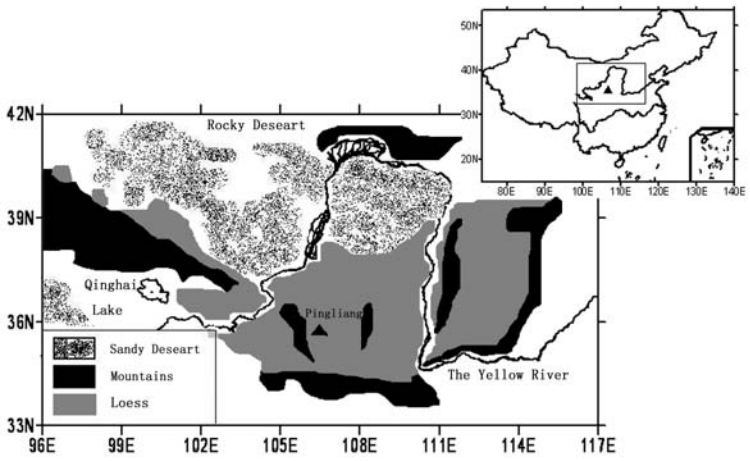

Fig. 1. Geomorphic Regions of the Loess Plateau. (The triangle symbol indicates the location of the Pingliang Weather Station.)

economical development.

The forecasts of weather and climatic variation, influenced obviously by the energy and water exchange between the land and atmosphere, are very important in the Loess Plateau. At present, the experiments of land-atmosphere interaction and the researches of its influences on the monsoon season and climate have become very important parts in CLIVAR and GEWEX. In China, several large experiments have been conducted in the Tibetan Plateau and Northwest China. However, few surface flux and boundary layer measurements were fully conducted over the Loess Plateau. Yang et al. (2004) analyzed the surface energy balance in summer over the middle part in Gansu by using the field experimental data. The main studies have been focused on the variation of the vegetation and land evaporation by using remote sensing data and land process models in these regions (Zhan et al., 2004; Kimura et al., 2006; Zhao et al., 2006). Kimura et al. (2005) estimated the heat and water balances of the bare soil surface in the Loess Plateau by using a three-layer soil model. To improve the understanding of the land processes in the Loess Plateau, we conducted a pilot field experiment of the land-atmosphere interaction in Pingliang of the Gansu province from 26 August to 11 September 2004 (Wen et al., 2007). The data from different instruments are compared and corrected and the characteristics of energy exchanges were analyzed (Wei et al., 2005a). From July to September 2005, a formal Loess Plateau land-atmosphere interaction experiment (LOPEX05) including remote sensing, sounding and land-atmosphere interactions, was conducted in the same location as that of 2004. From April to September 2006, we conducted a supplementary experiment (LOPEX06) for vegetation-atmosphere interaction. The basic characteristics of the atmosphere and the boundary layer are expected to be understood by analyzing the data of the three experiments.

The vertical atmosphere is stratified by the profile of temperature with height. The tropopause is analyzed more because it is a promising fingerprint of the human effects on climate (Sausen and Santer, 2003). Some researches indicate that the greatest increases in the height of the tropopause have occurred in the extratropics in both hemispheres (Highwood et al., 2000; Randel et al., 2000; Santer et al., 2003). Anel et al. (2006) estimated changes in the height of the tropopause from 1973 to 1998 by using radiosonde data in the Eurasian region and indicated that the numbers of stations with positive trends are very sensitive to the quality of data and the methods used to remove inhomogeneities. The polar (first) and tropical (second) tropopauses over China are analyzed by using the sounding data and the results show: The height of the polar tropopause is about 9000–12000 m and the height of the tropical tropopause is about 15 000–17 000 m above the ground; the height of the polar tropopause obviously increased from 1969 to 1999 over Xinjiang in Northwest China (Zou et al., 1989; Zhang et al., 2005; Cai et al., 2006). Recently, Sohn and Ryu (2007) constructed the vertical profiles of seasonally varying pressure, temperature, water vapor, and trace gases over the East Asia region and analyzed the optical characteristics of the East Asia reference atmospheres.

The vertical structure of the atmospheric boundary layer (ABL) has a considerable influence on meteorological and environmental issues. The ABL height is an essential parameter in atmospheric dispersion modeling and controlling the extent of the vertical mixing of pollutants near the surface. At present, many ad-

vanced instrumentations (lidar, sodar, wind profilers etc.) may provide accurate data for analyzing ABL (Grimsdell and Angevine, 1998; Emeisa et al., 2004). Seibert et al. (2000) reviewed the different methods for determining the ABL heights. Wu and Dong (1998) estimated the ABL heights over China using radiosonde data from 125 weather stations and showed that the ABL heights in western China are higher than those in the eastern China. Recently, the research on the boundary layer characteristics of temperature and humidity focused on the Tibetan Plateau, the Hexi Corridor and some big megalopolises in China (Li et al., 2000; Liu and Miao, 2001; Liu et al., 2002; Lu et al., 2002; Zhang et al., 2003; Ao et al., 2004), but little researches on the boundary layer over the Loess Plateau have been reported so far.

In this paper, we analyze the atmosphere sounding data collected during LOPEX05 and obtain the atmospheric vertical structure and the boundary layer characteristics of temperature and humidity in late summer on clear days over the east Gansu loess plateau. The objective of this study is to improve our understanding of the atmospheric structure over the Loess Plateau.

2. Data and methodology

The atmospheric sounding was conducted 12 times in two days. The observation location is at the Pingliang Weather station (35°33′N, 106°40′E, 1348 m height) located at the north suburb of Pingliang City and to east of the Liupanshan Mountain (see Fig. 1).

The sounding apparatus used in the experiment is the Tape59-701 Mechanical Radiosonde and Secondary Windfinding Radar, which has been used in other operational soundings by the Pingliang Weather Station of the China Meteorological Administration. Two clear days, 23 August and 2 September, were selected for the sounding observation. There are 6 different times for each 3 hours interval from 0800 to 2300 LST every day respectively. The local time in Pingliang is about 40 minutes later than that of Beijing Time. The sounding heights are from the ground up to about 20 000 m above the ground surface and have reached up to 27 000 m of the lower layer of the stratosphere at some times. The sounding observation includes elevation, azimuth, and slant range of the small balloon and codes of air temperature, relative humidity and air pressure.

The vertical resolution is influenced by the sampling rate and the ascending speed of the sounding balloon. To obtain higher resolutions, the sampling rate should be as high as possible and the ascending speed should be as slow as possible. The ascending speed of the balloon increases, as it gets higher because the pressure decreases. The wind rate and direction are computed from the data of the elevation, azimuth, and slant range. Because the sampling rate is only one time per minute for the elevation, azimuth, and slant range, the vertical resolution for the wind varies from 40 m at lower altitudes to 300 m at higher altitudes. The codes of temperature, humidity and pressure are received about 8 times every minute. The codes are converted to the real values by the fitted lines of the radiosonde critical certificates. Their vertical resolution is higher than that of wind and varies from 5 m at lower altitudes to 50 m at higher altitude.

The quality control of the data is especially important to the upper-air measurements. The Tape59–701 Mechanical Radiosonde and Secondary Windfinding Radar is being abandoned in China because of its relative low precision. Now, it is only used in a few stations for the upper air-soundings. To guarantee the quality of the data, the 59–701 data process system was established by the Chinese Meteorological Administration in 2000. In this investigation, we have paid special attention in conducting the quality controls of the data. These controls mainly include corrections in the codes and the calibration by using surface pressure, the temperature of the dry and wet bulbs as well as the radiation calibration.

The operating wave length of the Tape59-701 Mechanical Radiosonde and Secondary Windfinding Radar is 75 cm. The measurement maximal height, angular measurement precision and the slant range error are respectively is 30 km, 0.15°–0.2° and 80 m. The measurement error of the wind correlates with the precision and synchronization of the elevation, azimuth, and slant range. The errors of the wind direction and the azimuth are equivalent when it varies less. The mean square deviation of the wind speed is about 0.5–1.2 m s^{-1} below 10 km and 1.2–3.0 m s^{-1} from 10 to 20 km above the ground (Zhang, 1982; Li, 1987). The measurement error of air temperature is ±0.28°C between 1000 hPa and 500 hPa, ±0.42°C between 500 hPa and 200 hPa, ±1.0°C between 200 hPa and 10 hPa; the measurement error of air pressure is ±2.1 hPa between 1050 hPa and 10 hPa; the measurement error of relative humidity is ±2% (Zou et al., 2006). By these data, the potential temperature, specific humidity, dew-point, height above the ground, air density and vapor density are obtained according routine formulas. The measurement error of the height is 10–20 m below 10 km and 50–100 m from 10 to 20 km above the ground (Li, 1987). Several profiles and tables of wind, temperature and humidity will be plotted and analyzed and the boundary layer characteristics will be analyzed by this data in the following sections.

3. The characteristics of atmospheric in the late summer over the east Gansu loess plateau

The profiles including air temperature, potential temperature, dew-point, specific humidity, vapor density, relative humidity, wind speed and wind direction have been plotted and analyzed in this investigation. Two profiles (see Fig. 2) at 0800 LST on 23 August and at another 1400 LST on 2 September are selected as examples to illustrate the general characteristics of the vertical structure of the atmosphere.

Figure 2a shows the vertical variation of the air temperature, the potential temperature, and the dew-point. It is evident that there is a turning point at about 16 000 m above the ground. The air temperature and the dew-point are both decreasing from the ground to the turning point and then increasing above the turning point. In other words, the air temperature and the dew-point both reach a minimum value at the turning point. The potential temperature gradient has a jump near the turning point. According to the WMO Thermodynamic Definition, the height of the tropopause is the lowest height at which the lapse rate decreases to 2°C km^{-1} or less provided also that the average lapse rate between this height and all higher altitudes within 2 km does not exceed 2°C km^{-1} (Anel et al., 2006). We found that the height of the tropopause is about 15 000 m above ground surface at 0800 LST on 23 August and lower than one of the turning point. Zou et al. (1989) pointed out that the southern border of the polar tropopause had receded to 38°–40°N in August. Hence, the tropopause analyzed here by us is the tropical (second) one over Pingliang and its height is accordant to the some research results (Cai et al., 2006). We regard the height of the turning point as the bottom of the stratosphere here to denote its difference to the tropopause.

At the bottom of the stratosphere, the vapor density and the relative humidity both become quite low and the specific humidity reaches its minimum (see Fig. 2b). Figure 2c shows the vertical variation of the wind speed and direction. The wind speed also reaches its minimum and the wind direction changes from northwest to eastward at the bottom of the stratosphere.

The properties of the profiles for all 12 soundings on 23 August and 2 September are investigated. The characteristics derived from the two examples exist at every time. The minimum values of the air temperature and the dew-point and the corresponding heights at the bottom of the stratosphere are summarized in Table 1. Other variables such as pressure, specific humidity, relative humidity, potential temperature, va-

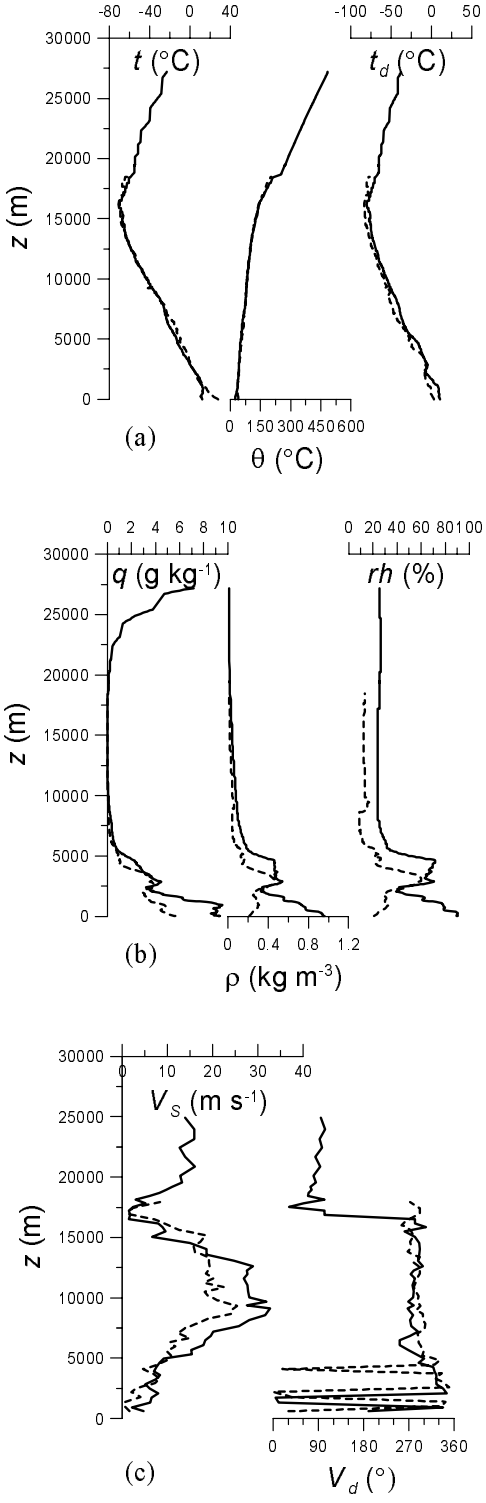

Fig. 2. Vertical profiles at 0800 LST on 23 August (solid lines) and at 1400 LST in 2 September (dashed lines) over the Pingliang Weather Station (a) air temperature (t), potential temperature (θ) and dew-point (t_d); (b) specific humidity (q), vapor density (ρ) and relative humidity (rh); (c) wind speed (V_s) and wind direction (V_d) (note: z indicates height above ground surface).

Table 1. Minimums of the air temperature, the corresponding heights, and the other variables at the bottom of stratosphere.

Date	Time (LST)	$T_{\min}$ (°C)	$T_{\mathrm{d,min}}$ (°C)	H (m)	P (hPa)	q (g kg^{-1})	rh (%)	θ (°C)	ρ (k gm^{-3})	ρ_{a} (k gm^{-3})
23 Aug	0800	−71.2	−80.2	16171	81.9	0.01	24.2	141.4	0.03	0.14
	1100	−68.4	−79.1	16296	80.4	0.01	19.4	149.4	0.03	0.14
	1400	−68.2	−81.5	16044	83.5	0.01	12.6	145.3	0.02	0.14
	1700	−64.5	−77.4	16856	73.4	0.01	14.7	169.9	0.02	0.12
	2000	−70.1	−84.6	16394	78.9	0.00	9.8	148.2	0.01	0.14
	2300	−72.0	−82.5	16538	77.0	0.00	18.7	146.7	0.03	0.13
2 Sep	0800	−72.3	−81.0	16172	82.7	0.01	25.2	138.0	0.04	0.14
	1100	−69.9	−79.9	15218	95.5	0.01	21.1	126.1	0.03	0.16
	1400	−70.6	−83.7	16303	80.8	0.00	12.3	144.4	0.02	0.14
	1700	−70.3	−81.3	17807	63.6	0.01	17.8	174.5	0.02	0.11
	2000	−70.0	−82.0	17487	66.8	0.01	15.1	169.0	0.02	0.11
	2300	−68.2	−76.9	14182	112.9	0.01	27.0	110.6	0.05	0.19

Note: $T_{\min}$—minimums of air temperature, $T_{\mathrm{d,min}}$—minimums of dew point, H–height above ground surface, P—pressure, q—specific humidity, rh—relative humidity, θ—potential temperature, ρ—vapor density, ρ_{a}—air density.

por density and air density at the corresponding heights are also summarized in Table 1. The minimums of the air temperature and the dew-point occur at about 16 500 m and vary between 14 000 m and 18 000 m above the ground, this height is regarded as the bottom of the stratosphere. Obviously, there is a little difference in the heights for the bottom of the stratosphere in consesecutive hours on 23 August or 2 September. The errors in the bottom of the stratosphere are brought mainly from the vertical resolution and measurement precision of the height. The vertical resolution is about 50 m for the temperature data at the bottom of the stratosphere. The measurement error of the height is about 100 m from 10 to 20 km above the ground (Li, 1987). So, the error of the bottom of stratosphere is about ±150 m. The air temperature varies between −64°C and −72°C at different times; the dew-point between −77°C and −85°C, and the potential temperature between 110°C and 175°C. The air is quite dry there and the relative humidity is less than 25%. The specific humidity has been as low as 0.01 g kg^{-1}. The vapor density is less than 0.05 kg m^{-3}. The air density is less than 0.19 kg m^{-3}. At the bottom of stratosphere, the measurement error of the air temperature, pressure and relative humidity is ±1.0°C, ±2.1 hPa and ±2% respectively (Zou et al., 2006). The hour-to-hour differences in the air temperature are less than or close to the error, but the hour-to-hour differences of the dew-point, pressure, relative humidity and the heights for the bottom of the stratosphere are obviously larger than the error except for one or two soundings and might be attributed mainly to the variation of the weather conditions.

It is evident in Fig. 2c that the north-west or the north wind dominates the troposphere above the boundary layer over the Pingliang region. A maximum wind rate of about 30 m s^{-1} is found at approximately 10000 m above the ground in the upper troposphere. It is known that the westerly belt dominates the middle and high latitudes in the Northern Hemisphere. Obviously, the maximum wind is the westerly jet. Its values at all 12 soundings are listed in Table 2. It is stronger but the corresponding height is lower on 23 August than 2 September. The maximum values of wind speed vary between 33 m s^{-1} and 36 m s^{-1} and the corresponding heights vary between 8300 m and 10 400 m above the ground on 23 August. The maximums of the wind speed vary between 25 m s^{-1} and 31 m s^{-1} and the corresponding heights vary between 9300 m and 14 300 m above the ground on 2 September. The wind direction of the westerly jet turns

Table 2. Maximum wind speeds of the westerly jet, the corresponding heights above ground surface and the wind directions.

Date	Time (LST)	Wind maximum (m s^{-1})	Height (m)	Wind direction (°)
23 Aug	0800	32.6	9121	267
	1100	35.0	8371	279
	1400	34.1	9006	280
	1700	36.4	8515	282
	2000	34.0	10431	293
	2300	34.8	8595	298
2 Sep	0800	28.3	12663	297
	1100	27.1	9685	304
	1400	25.3	9339	293
	1700	28.9	10992	293
	2000	24.8	14333	259
	2300	31.0	10023	290

Table 3. The maximums of the relative humidity, the corresponding heights, air pressure and other moisture variables.

Date	Time (LST)	Relative humidity maximum (%)	Height above ground (m)	Pressure (hPa)	Vapor density (kg m^{-3})	Specific humidity (g kg^{-1})
23 Aug	0800	70.6	2877	605	0.54	4.5
	1100	62.4	2942	600	0.49	4.2
	1400	52.6	2780	612	0.41	4.0
	1700	57.8	3113	589	0.55	3.6
	2000	72.3	3011	593	0.55	4.4
	2300	67.2	2725	616	0.54	4.9
2 Sep	0800	73.3	3569	556	0.53	3.5
	1100	67.3	2870	606	0.52	4.4
	1400	60.0	3136	587	0.46	3.8
	1700	69.4	2986	598	0.53	4.5
	2000	60.8	2908	604	0.47	4.2
	2300	55.2	2533	636	0.44	4.1

to 260° and 305°. The measurement error is about 1.2 m s^{-1} for the wind speed and 0.2° for the wind direction in Table 2. The westerly jet is relatively stable on 23 August and 2 September over the region.

Another explicit characteristic about the vertical structure of the atmosphere over the Pingliang region in the late summer is that an inverse humidity layer occurs at about 3000 m above the ground (see Fig. 2b), as shown respectively in the profiles of the relative humidity, vapor density and specific humidity, respectively. It should be the major vapor transport path in the middle and low troposphere in this region. The maximum values of the relative humidity and the corresponding heights, pressure and other moisture variables at all 12 soundings are listed in Table 3. The corresponding heights of the maximum vapor values vary between 2500 m and 3600 m above the ground. The relative humidity varies between 50% and 75%, the vapor density varies between 0.4 kg m^{-3} and 0.6 kg m^{-3}, and the specific humidity varies between 3.5 g kg^{-1} and 5.0 g kg^{-1}. The cloud cover is less than 0.3 on 23 August and 2 September and the inverse humidity layer occurs at all times of soundings, but the cloud occurs only occasionaly. The main factor to form the inverse humidity layer between 2500 m and 3600 m height above the ground is not due to cloud. We will investigate the causes in a new field observation experiment. The inverse humidity layer might be related to the Liupanshan Mountain, where is one of the causes to make much hail weather occurs in the summer in Pingliang region.

In summary, the bottom of the stratosphere is at about 16 500 m and varies between 14 000 m and 18 000 m above the ground. Near the bottom of the stratosphere, the air temperature, the dew-point, and the specific humidity reach a minimum value; the gradient potential temperature has a jump; the vapor density and the relative humidity both become quite low; the wind speed also has a minimum value and the wind direction changes from northwest to eastward near the bottom of the stratosphere. It is shown in Fig. 2c that the north-west or the north wind dominates the troposphere above the boundary layer. A maximum wind speed of about 30 m s^{-1} is found at about 10 000 m above the ground in the higher troposphere. The center of the westerly jet is located between 8300 m and 14 300 m above the ground and varies from 25 m s^{-1} to 36 m s^{-1}. The wind direction of the westerly jet ranges between 260° and 305°. There is an inverse humidity layer at about 3000 m height above the ground.

4. Variation of the air temperature and moisture within the boundary layers in late summer over the east Gansu loess plateau

Figure 3 shows the profiles of the potential temperature and the specific humidity in the layer below 1400 m height on 23 August. Although the vertical sampling resolutions are coarse, some phenomena can still be evident.

In Fig. 3a, the air potential temperature increases gradually from 0800 to 1700 LST and decreases from 1700 to 2300 LST; the maximum of the air temperature occurs at 1700 LST in the layer below 800 m; the ground surface air temperature inversion in the surface layer occurs at at 0800, 2000, and 2300 LST and shows that the stable boundary layer (SBL) occurs at night or in the morning; the convective boundary layer (CBL) occurs in the daytime and appears higher in the afternoon; the inversion layer (IL) above the CBL is relatively thick.

In Fig. 3b, the variation of the specific humidity is more complex than that of the potential temperature; the vapor increases from 0800 to 1400 LST and varies slowly from 1400 to 2300 LST in the layer near the ground surface layer below 150 m; the surface humid-

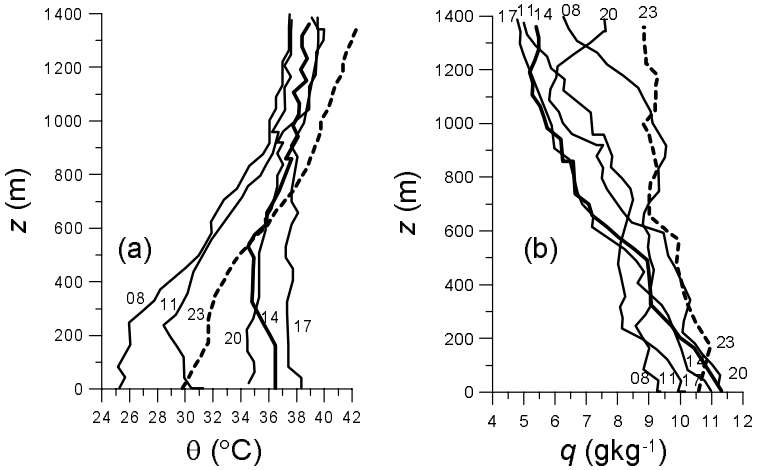

Fig. 3. Profiles of (a) the potential temperature and (b) the specific humidity, (b) in the layer below 1400 m height on 23 August 2005. (The numbers show Beijing Time. The thick solid lines are at 14. The dashed lines are at 23.)

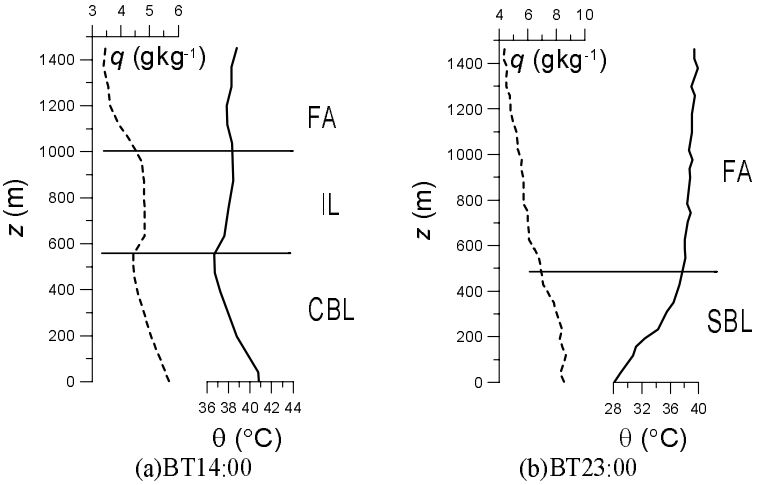

Fig. 4. Profiles of the potential temperature (the solid lines) and the specific humidity (the dashed lines) in the layer below 1500 m height on 2 September 2005. (FA-free atmosphere layer, SBL-stable boundary layer, CBL-convective boundary layer, IL-inversion layer)

ity inverse occurs obviously at 2300 LST; the maximum of the vapor occurs at 1100 LST and the minimum at 2000 or 2300 LST in the layer from 200 m to 500 m; the maximum of the vapor occurs at 1400 LST from 700 m to 1200 m and at 1700 LST from 1200 m to 1400 m; the minimum occurs at 0800 LST in the layer from 700 m to 1000 m and at 2300 LST in the layer from 1000 m to 1400 m. The time that the maximum vapor occurs is not same for the different layers.

At 0800 LST after the sunrise at 0618 LST, the convection develops below 100 m and invades the low part of the SBL that formed during the night. At noon (1400 LST, the thick solid lines in Fig. 3), the IL occurs in the layer from 550 m to 1000 m above the ground and convection develops below 550 m. At 2300 LST (the dashed lines in Fig. 3), the SBL occurs in the lower layer and has develops up to about 650 m. The measurement error of the height is 10–20 m below 10 km height above ground surface (Li, 1987). The vertical resolution is 5–10 m at this layer. The error of the boundary layer height is about ±30 m.

The convection is less active and the depth of the ABL is smaller on 2 September than that on 23 August. Figure 4 shows profiles of the potential temperature and the specific humidity in the layer below 1500 m at 1400 and 2300 LST on 2 September 2005. At

the noon (1400 LST, Fig. 4a), the IL is from 550 m to 1000 m. At 2300 LST (Fig. 4b), the SBL reaches to about 490 m.

By the analysis of the boundary layer structure on 23 August and on 2 September, we conclude that the height of the ABL reaches about 1000 m and the height of the SBL reaches to 650 m in late summer in the Pingliang region. This conclusion is educed only by the variation of the air temperature and humidity and need to be validated by other data. Because the wind data has a coarse resolution in the lower layer, it can not be used to analyze the variation of the atmospheric boundary layer.

The boundary layer characteristics of the Pingliang region are quite different from those in arid regions and the Tibetan Plateau in China. The height of the ABL can reach 3600 m and the depth of the SBL can only reach 190 m in the summer over the Jinta region located in the Hexi Corridor in the Northwest China (Wei et al., 2005b). The height of the ABL could reach as high as 2750 m in the summer over the Tibetan Plateau (Liu et al., 2002; Zhang et al., 2003). The height of the boundary layer is far lower over the Loess Plateau than that over the arid region in Northwest China and also lower than that in the Tibetan Plateau. It might be caused by a lower sensible heat flux from the ground to the air.

5. Conclusions

By the above results from our analysis, the following atmospheric characteristics of late summer clear days are drawn from over the Loess Plateau:

The bottom of the stratosphere is at about 16 500 m and ranges between 14 000 m and 18 000 m above the ground. Near the bottom of the stratosphere, the air temperature, the dew-point and the specific humidity have a minimum value; the gradient of potential temperature has a jump; the vapor density and the relative humidity both become quite low; the wind rate also has a minimum value and the wind turns from northwest to eastward near the bottom of the stratosphere. The center of the westerly jet is located between 8300 m and 14 300 m above the ground and the intensity varies between 25 m s^{-1} and 36 m s^{-1}. The wind direction of the westerly jet varies between 260° and 305°. There is an inverse humidity layer at about 3000 m height above the ground. It should be the main vapor transport path in the middle and lower troposphere over the Loess Plateau.

The maximum of the air temperature occurs at 1700 LST in the layer below 800 m above ground. The inversion layer is relatively thick. The time that the maximum vapor occurs is not the same for different layers. The depth of atmospheric boundary layer can reach about 1000 m and the depth of the stable boundary layer can reach to 650 m. The depth of the boundary layer is much lower over the Loess Plateau than that over the arid region in the Northwest China and also lower than that of the Tibetan Plateau.

Acknowledgements. This research is funded by the Centurial Program sponsored by the Chinese Academy of Sciences (Grant No. 2004406), the Project KZCX2-YW-220, Program of Knowledge Innovation for the 3rd period of the Chinese Academy of Sciences, the National Natural Science Foundation of China (Grant No. 40730952) and the Field Station Foundation of the Chinese Academy of the Sciences.

REFERENCES

Anel, J. A., L. Gimeno, L. Torre, and R. Nieto, 2006: Changes in tropopause height for the Eurasian region determined from CARDS radiosonde data. *Naturwissenschaften*, **93**, 603–609. doi: 10.1007/s00114-006-0147-5.

Ao, Y. H., S. H. Lu, and Y. C. Chen, 2004: Characteristic analysis of different terrain PBL in Hexi Region. *Plateau Meteorology*, **23**(2), 215–219. (in Chinese)

Cai, F., J. Li, H. Q. Ming, B. Liu, and H. B. Yu, 2006: Climatic characteristics of tropopause over Shenyang. *Journal of Meteorology and Environment*, **22**(1), 11–16. (in Chinese)

Doug, K., 1997: Who will feed China? *Journal of Soil and Water Conservation*, **52**, 398–399.

Emeisa, S., M. Christoph, V. Siegfried, W. J. Mullerd, and K. Schafer, 2004: Atmospheric boundary-layer structure from simultaneous SODAR, RASS, and ceilometer measurements. *Atmos. Environ.*, **38**, 273–286.

Grimsdell, A. W., and W. M. Angevine, 1998: Convective boundary layer height measurement with wind profilers and comparison to cloud base. *J. Atmos. Oceanic Technol.*, **15**, 1331–1338.

Highwood, E. J., B. J. Hoskins, and P. Berrisford, 2000: Properties of the arctic tropopause. *Quart. J. Roy. Meteor. Soc.*, **126**, 1515–1532.

Kimura, R., Y. Liu, N. Takayama, X. Zhang, M. kamichika, and N. Matsuoka, 2005: Heat and water balances of the bare soil surface and the potential distribution of vegetation in the Loess Plateau, China. *Journal of Arid Environments*, **63**(2), 439–457.

Kimura, R., J. Fan, X. C. Zhang, N. Takayama, M. kamichika, and N. Matsuoka, 2006: Evapotranspiration over the grassland field in the Liudaogou basin of the Loess Plateau, China. *Acta Ocologica*: *International Journal of Ecology*, **29**(1), 45–53.

Li, B. J., 1987: Synchronization and simultaneity of the measurement and wind error on the 701 Radar. *Meteorological Monthly*, **13**(12), 42–44. (in Chinese)

Li, J. L., Z. X. Hong, and S. F. Sun, 2000: An observational experiment on the atmospheric boundary layer in Gerze Area of the Tibetan Plateau. *Chinese J. Atmos. Sci.*, **24**(3), 301–311. (in Chinese)

Liu, H. Y., and M. Q. Miao, 2001: Preliminary analysis on character isiics of boundary layer in Qinghai-Tibet Plateau. *Joural of Nanjing University* (*Natural Sciences*), **37**(3), 349–357. (in Chinese)

Liu, H. Z., H. S. Zhang, L. G. Bian, J. Y. Chen, M. Y. Zhou, X. D. Xu, S. M. Li, and Y. J. Zhao, 2002: Characteristics of micrometeorology in the surface layer in the Tibetan Plateau. *Adv. Atmos. Sci.*, **19**(1), 73–88.

Lu, L. H., L. G. Bian, Y. J. Cheng, Z. Q. Gao, and X. Wang, 2002: Obseravational study of wind and temperature profile of urban boundary layer in Beijing winter. *Journal of Applied Meteorological Sciences*, **13**(Suppl.), 13–25. (in Chinese)

Meng, X. M., and E. Derbyshire, 1998: Landslides and their control in the Chinese Loess Plateau: Models and case studies from Gansu Province, China. *Geohazards in Engineering Geology*, **15**(1), 141–153.

Randel, W. J. , F. Wu, and D. J. Gaffen, 2000: Interannual variability of the tropical tropopause derived from radiosonde data and NCEP reanalysis. *J. Geophys. Res.*, **105**, 15509–15524.

Santer, B. D., and Coauthors, 2003: Behavior of tropopause height and atmospheric temperature in models, reanalyses, and observations: Decadal changes. *J. Geophys. Res.*, **108**, 4002, doi: 10.1029/2002JD002258.

Sausen, R., and B. D. Santer, 2003: Use of changes in tropopause height to detect human influences on climate. *Meteor. Z.*, **12**, 131–136.

Seibert, P., F. Beyrich, S. Gryning, S. Joffre, A. Rasnussen, and P. Tercier, 2000: Review and intercomparison of operational methods for the determination of the mixing height. *Atmos. Environ.*, **34**, 1001–1027.

Seth, C., F. R. Li, and H. L. Wei, 2000: Rainwater harvesting agriculture in Gansu Province, PRC. *Journal of Soil and Water Conservation*, **55**, 112–114.

Sohn, B. J., and G. H. Ryu, 2007: Seasonally varying reference atmospheres for East Asia. *Adv. Atmos. Sci.*, **24**(2), 181–190. doi: 10.1007/s00376-007-0181-z.

Wei, Z. G., J. Wen, S. H. Lu, S. Q. Chen, Y. H. Ao, and L. Liang, 2005a: A primary field experiment of land-atmospheric interaction and ground surface energy in clear day over the loess plateau. *Plateau Meteorology*, **24**(4), 494–497. (in Chinese)

Wei, Z. G., and Coauthers, 2005b: A primary research on the characteristics of wind, temperature and humidity in the boundary layer over Jinta in summer. *Plateau Meteorology*, **24**(6), 846–856. (in Chinese)

Wen, J., Z. G. Wei, S. H. Lu, S. Q. Chen, Y. H. Ao, and L. Liang, 2007: The Autumn daily characteristics of land surface heat and water exchange over the Loess Plateau Mesa in China. *Adv. Atmos. Sc.*, **24**(2), 301–310. doi: 10.1007/s00376-007-0301-9.

Wu, Z. C., and B. Q. Dong, 1998: Geographical distribution and seasonal variation of atmospheric maximum mixing depth over China. *Bulletin of Sciences and Technology*, **14**(3), 158–163. (in Chinese)

Yang, X. G., Q. Zhang, R. Y. Wang, P. L. Ma, T. G. Yang, and H. Y. Liu, 2004: Experimental study on surface energy balance over Loess Plateau of middle part Gansu in summer. *Plateau Meteorology*, **23**(6), 828–834. (in Chinese)

Yang, W. Z., and M. G. Shao, 2000: *Soil Water Research ' in China's Loess Plateau.* Science Press, Beijing, China, 4–10. (in Chinese)

Zhan, Z. M., Z. D. Feng, and Q. M. Qin, 2004: Study on land surface evapotranspiration on remote sensing data on Longxi Loess Plateau of China. *Geography and Geo-information Science*, **20**(1), 16–19. (in Chinese)

Zhang, C., 1982: Choose to the windfinding methods and error analysis on the 701 Radar. *Meteorological Monthly*, **8**(8), 25–26. (in Chinese)

Zhang, G. X., J. Li, C. X. Cui, and Y. Xin, 2005: Change trend and analysis of abrupt change for the first tropopause height over Xinjiang in 1960–1990. *Advances in Climate Change Research*, **1**(3), 106–110. (in Chinese)

Zhang, G. Z., X. D. Xu, and J. Z. Wang, 2003: A dynamic study of Ekman characteristics by using 1998 SCSMEX and TIPEX boundary layer data. *Adv. Atmos. Sci.*, **20**(3), 349–356.

Zhao, D. M., B. K. Su, and M. Zhao, 2006: Soil moisture retrieval from satellite images and its application to heavy rainfall simulation in eastern China. *Adv. Atmos. Sci.*, **23**(2), 299–316. doi: 10.1007/s00376-006-0299-4.

Zou, J. S., J. Q. Zhang, and B. Z. Wang, 1989: The characteristics of temporal and spatial variation of tropopause over China and its controlling factors. *Scientia Meteorologica*, **9**(4), 417–426. (in Chinese)

Zou, Y. L., X. Wang, F. J. Gao, and Q. L. Lu, 2006: Compare and analysis on the measurement data between the L band and the 59–701 sounding system. *Shandong Meteorology*, **26**(2), 49–50. (in Chinese)